

Received August 4, 2018, accepted October 6, 2018, date of publication October 25, 2018, date of current version November 14, 2018.

Digital Object Identifier 10.1109/ACCESS.2018.2877477

Non-Orthogonal Multiple Access With Sequence Block Compressed Sensing Multiuser Detection for 5G

MEHMOOD ALAM^{1,2}, (Student Member, IEEE), AND QI ZHANG¹, (Member, IEEE)

¹Department of Engineering, Aarhus University, 8200 Aarhus, Denmark

²National University of Sciences and Technology, Islamabad 44000, Pakistan

Corresponding author: Mehmood Alam (mehmood.alam@eng.au.dk)

This work was supported in part by Aarhus University, Denmark, and in part by the National University of Sciences and Technology, Pakistan.

ABSTRACT Compressed sensing-based multiuser detection (CSMUD) is a promising candidate to enable grant-free non-orthogonal multiple access for massive machine-type communication in the fifth-generation (5G) wireless communication system. Exploiting the sporadic node activity of the massive machine-type communication, CSMUD recovers the signal from far fewer linear measurements than the number of users, thereby facilitating massive connectivity. However, with the increase in the number of sensor nodes, the errors in the activity detection also increase. In this paper, we propose sequence block-based compressed sensing multiuser detection (SB-CSMUD), which enhances the activity detection by using block of multiple spreading sequences as signature of the node. It is demonstrated both empirically and theoretically that the SB-CSMUD scheme besides improving the detection error rate also increases the spectrum efficiency. Simulation results show that for the same least square estimation error rate (LSER), SB-CSMUD not only reduces the bandwidth by 10% but also reduces the bit error rate by more than 1.5 order of magnitude at signal-to-noise ratio (SNR) of 15 dB. The bandwidth can even be reduced by 25%–30% at SNR > 20 dB for achieving the same detection error rate at the cost of LSER. Furthermore, owing to the diversity in the spreading, the proposed scheme provides a more homogeneous performance for all the nodes. In addition, the computational complexity of the SB-CSMUD is the same as that of CSMUD at the only expense of the memory requirement for hosting the block sequence at the node.

INDEX TERMS Massive MTC, grant free medium access, NOMA, compressive sensing multiuser detection, system overloading.

I. INTRODUCTION

Massive machine type communication (mMTC) is one of the important communication services in the future 5G wireless communication system. It has a great potential in a wide range of applications such as in monitoring, logistics, smart grids, smart cities and so on. Different from the human driven communication, the mMTC is characterized by low data rate and sporadic activity [1]. It is estimated that the number of connected devices will rise to 50 billion by 2020 [2] and even up to 500 billion by 2024 [3]. The abundance of such devices poses enormous challenges to meet the performance requirements such as high spectral efficiency, massive connectivity and low power consumption of the 5G communication system [4], [5]. The current cellular systems such as 3GPP long term evolution (LTE) [6] is primarily designed for human centric communication which is characterized by

high data rates. The control signaling overhead for medium access of the LTE protocols is much higher as compared to the mMTC payload, which makes the LTE highly inefficient to cope with the mMTC traffic [7], [8]. Furthermore, the current orthogonal multiple access (OMA) schemes are based on orthogonal resource allocation which are not capable to accommodate the huge number of devices due to the orthogonality constraint. The peculiar characteristics of the mMTC traffic demands for a paradigm shift of the current multiple access scheme to reduce the control signaling overhead and to accommodate massive number of nodes.

Non-orthogonal multiple access (NOMA) has become a key technique to meet the performance requirements of the mMTC in 5G wireless communication system. In NOMA schemes, unlike the conventional OMA schemes, non-orthogonal resources are assigned to the users.

The non-orthogonality allows the multiple access scheme to be overloaded, i.e., facilitating multiple users to share the available resources.

A. RELATED WORK

Various schemes have been proposed in the literature that uses the NOMA principal. These schemes can be divided into two main categories: the power domain NOMA and the code domain NOMA. In the power domain NOMA, the non-orthogonality is introduced by allocating different power levels to the users [9]. The power levels are unique for each user and serve as signatures in the multiuser detection which is carried out by using successive interference cancellation (SIC) [10].

In code domain NOMA, non-orthogonal codes are used to spread the data. At the receiver, advanced multiuser detection techniques such as message passing algorithm [11] and SIC are used to separate the users. Different variants of the code domain NOMA are present in the literature, the most promising of which are sparse code multiple access (SCMA) [12]–[14], pattern division multiple access (PDMA) [15], multi-user shared access (MUSA) [16] and so on. In SCMA, the information bits after channel coding are directly mapped to user specific sparse codewords and message passing algorithm is used at the receiver for multiuser detection. The PDMA considers each user's channel state and accordingly allocates a different number of non-zero elements to the codeword. The MUSA is a sequence based NOMA scheme that assigns low correlated spreading sequences to the nodes and uses SIC for multiuser detection.

Compressive sensing based multiuser detection (CSMUD) [17]–[21] is a recently proposed scheme to enable grant-free non-orthogonal code division multiple access (CDMA) for sporadic mMTC in 5G. Compressed sensing is a signal processing technique in which a sparse signal is sampled at low rate and is reconstructed by solving underdetermined linear systems. In mMTC, the CSMUD exploits the sparsity in the activity of the nodes. Many variants of CSMUD have been proposed in the recent years to efficiently handle the massive connections. In [17], for the first time sparsity-exploiting algorithms based on maximum *a posteriori* probability criterion for CDMA multiuser detection are proposed. However, besides the higher complexity of the convex optimization based algorithms, they are not able to efficiently support more users than the orthogonal resources.

In [18], the greedy algorithms, e.g., orthogonal matching pursuit (OMP) [22] and orthogonal least square (OLS) [23], are used for CSMUD to reduce the computational complexity and to support the overloaded systems, i.e., the system having more users than orthogonal resources. The performance of the OLS based CSMUD is further improved in [24] by exploiting the group sparsity of the multiuser symbols. It is assumed that when a node is active, it transmits a sequence of symbols, thereby, making the multiuser signal group sparse. The performance enhances for the reason that the activity detection

considers multiple symbols which are individually affected by random noise.

Another challenge in CSMUD is that the number of supported nodes are limited by the number of dedicated signatures. In [25] to increase the number of supported nodes, a contention based medium access scheme is proposed in which each node randomly selects a sequence set from a predefined pool of sequence sets. At the receiver, the nodes are identified by the user IDs which are embedded within the data frame. However, as compared to the non-contention based medium access, additional errors are caused by the collision in medium access. In addition, the activity detection is dependent on the accurate estimation of the signal, which requires higher SNR and higher sparsity.

Monsees *et al.* [19] propose multicarrier compressed sensing multiuser detection in which CSMUD is applied to orthogonal subcarriers combined with CDMA. The proposed scheme improves the spectral efficiency and the flexibility in accessing the time-frequency resources. A variant of the OMP algorithm called group orthogonal matching pursuit (GOMP) is used which exploits the group sparsity of the signal. Instead of using a single symbol the whole frame is used for activity detection which improves the detection error rate (DER).

The performance of the CSMUD depends on the correlation between the spreading sequences, the higher the correlation is, the higher the DER will be. With the increase in the number of nodes, the correlation between the spreading sequences increases which consequently degrades the DER. For a fixed number of spreading sequences, the correlation between them is dependent on the spreading factor, i.e., the length of the spreading sequences. However, to reduce the mutual correlation by increasing the spreading factor is spectrally inefficient.

B. MAIN CONTRIBUTIONS

In this paper, we have proposed the SB-CSMUD scheme in which a block of sequences is assigned to each node instead of assigning a single sequence. The sequence blocks are designed such that each node has a unique sequence block which serves as the signature of the node. The activity detection is based on the maximum mutual correlation of the sequence blocks instead of the maximum mutual correlation between single sequences. In SB-CSMUD, the maximum correlation between the signatures of the nodes becomes smaller for the reason that the correlations are averaged over multiple spreading sequence in a block. The main contributions of the paper are as follows:

- Keeping the same least square estimation error rate (LSER), a 10% gain in the bandwidth is achieved along with a reduction of 1.5 order of magnitude in the BER at SNR = 15 dB. The bandwidth can further be reduced by 25% – 30% to achieve the same DER at the cost of increased LSER.
- A more homogeneous performance in terms of LSER of all nodes is achieved as compared to

CSMUD. Thanks to the diversity introduced by the multiple sequences in a sequence block.

- Capability to support more simultaneously active nodes is obtained. It is shown that for SNR = 20 dB, SB-CSMUD can support 50% more active nodes than CSMUD.
- Bound of performance metric for the SB-CSMUD is derived and it is shown that probability of successful support recovery of the proposed SB-CSMUD is higher than that of the conventional CSMUD.
- Extensive simulations are carried out to investigate the effect of different parameters such as the frame size, sequence block size and sparsity.

In the proposed scheme, the nodes are required to store the sequence blocks, therefore, the memory requirement of the node is slightly increased, however, the computational complexity of the SB-CSMUD is same as that of the CSMUD.

The paper is organized as follows. In Section II, the basic compressive sensing concept is described. Section III provides description of the system model and the CSMUD scheme. Section IV presents the proposed SB-CSMUD scheme and analytical derivation of the lower bound for the success probability of support recovery. In Section V, the simulation parameters are given and the performance of the proposed scheme is analyzed in detail. Finally Section VI concludes the paper.

Notations: In this paper, all boldface uppercase letters represent matrices such as \mathbf{A} , while all lowercase boldface letters represent vectors such as \mathbf{x} . The set of binary and complex numbers are represented by \mathbb{B} and \mathbb{C} , respectively. Italic letters such as k, x represent variables. Uppercase letters such as K and Greek letters such as γ represent a constant value.

II. COMPRESSIVE SENSING BASICS

Compressed sensing (CS) is a signal processing technique which samples a sparse signal at a rate much less than the Nyquist rate [26]. A signal $\mathbf{x} \in \mathbb{C}^{N \times 1}$ is said to be K -sparse if it has only K non-zero elements, $K \ll N$. The signal \mathbf{x} can be sparse with respect to any basis Φ . Let $\mathbf{z} = \Phi \mathbf{x}$ be a compressible signal with respect to Φ . The CS encoding process produces measurement $\mathbf{y} \in \mathbb{C}^{M \times 1}$ by a measurement matrix $\Psi \in \mathbb{C}^{M \times N}$, $K < M < N$,

$$\mathbf{y} = \Psi \Phi \mathbf{x} + \mathbf{n}, \quad (1)$$

where $\mathbf{n} \in \mathbb{C}^{M \times 1}$ is the background noise vector. The reconstruction of vector \mathbf{x} is to find a sparse vector $\hat{\mathbf{x}}$ which satisfies Equation (1). However, Equation (1) is an underdetermined system of equations which can be solved by using optimization techniques. The reconstruction of vector \mathbf{x} is formulated as

$$\hat{\mathbf{x}} = \arg \min_{\mathbf{x} \in \mathbb{C}^N} \|\mathbf{x}\|_0 \quad \text{subject to } \mathbf{y} = \Psi \Phi \mathbf{x}, \quad (2)$$

where $\|\cdot\|_0$ is the l_0 norm which simply gives the total number of non-zero elements in the vector. Equation (2) is a non-convex optimization problem, which is known to be NP-hard to solve. Certain relaxation approaches are used to solve Equation (2) such as, basis pursuit denoising in which the l_0 norm is relaxed to l_1 norm [27]. The l_1 minimization is a convex optimization problem which recovers the signal from an underdetermined system of equations with higher accuracy at the cost of complexity of cubic order. Another category of sparse signal reconstruction algorithms is greedy algorithms. In greedy algorithms, e.g., orthogonal matching pursuit (OMP), the support of $\hat{\mathbf{x}}$ is obtained iteratively by selecting the column of Ψ which has maximum correlation with the residual. The residual is initialized to \mathbf{y} and is updated in each iteration of OMP. Once the support is obtained, the corresponding data is estimated by using least square estimation. The greedy algorithms have lower complexity compared to the basis pursuit algorithms at the cost of a slight loss in the DER performance.

In order to successfully recover the signal using compressive sensing algorithms, the measurement matrix, Ψ , needs to satisfy the restricted isometry property (RIP) [28]. A matrix Ψ is said to satisfy RIP if there exists a constant $\delta_K \in (0, 1)$ such that for every K sparse signal, \mathbf{x} , [28]

$$(1 - \delta_K) \|\mathbf{z}\|_2^2 \leq \|\Psi \mathbf{z}\|_2^2 \leq (1 + \delta_K) \|\mathbf{z}\|_2^2. \quad (3)$$

Generally computing the restricted isometric constant, δ_K , is NP-hard. A Gaussian matrix is known to satisfy RIP with high probability whenever the number of rows scales linearly with the sparsity of the signal and logarithmically with the length of the signal [29], [30].

Another metric to evaluate the performance of a sensing matrix is the mutual coherence of the sensing matrix [31]. Mutual coherence is defined as the maximum correlation between the columns of the Ψ and can easily be computed as

$$\mu_{max} = \max_{1 \leq i \neq j \leq N} |\Psi_i^T \Psi_j| \quad (4)$$

where Ψ_i represents the i -th column of Ψ . In [32] it is shown that a matrix can recover the true support of the signal if the following condition of sparsity is satisfied.

$$K \leq \frac{1}{2} \left(\frac{1}{\mu_{max}} + 1 \right). \quad (5)$$

When the μ_{max} increases the number of supportable non-zero elements decreases. It is also shown in [33] and [34] that the mutual coherence provides acceptable performance guarantees.

III. COMPRESSIVE SENSING MULTIUSER DETECTION

A typical uplink mMTC scenario is illustrated in Figure 1, where N users are in the range of a base station (BS). Out of the N users, only a small fraction is active simultaneously. Considering a non-orthogonal multicarrier-CDMA (MC-CDMA) system [35] for uplink mMTC, each user is assigned with a spreading sequence to spread the data.

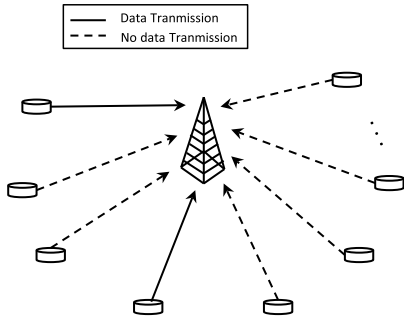


FIGURE 1. Massive machine type communication uplink scenario: N nodes connected to the base station.

The spreading sequence also serves as signature of the user. In the non-orthogonal MC-CDMA, the number of spreading sequences is more than the orthogonal resources, which introduces a correlation between the spreading sequences. Therefore, advanced multiuser detection techniques are required to recover the signal. In mMTC, since the multiuser signal is sparse, i.e., only few of the users are active, the multiuser detection can be posed as a compressive sensing problem, therefore, called compressive sensing multiuser detection (CSMUD).

The CSMUD is a joint detection of the activity and data. After detecting an active node the corresponding data is estimated using least square estimation. Therefore, the overall BER is dependent on the detection of both the activity and the data. Analytically, the overall BER is given as

$$BER = \frac{\xi L + (K - \xi)\gamma}{NL}, \quad (6)$$

where K is the number of simultaneously active nodes, L is the number of symbols in a frame, ξ is the number of errors in the activity detection and γ represents the average number of errors in the least square estimation.

The CSMUD is modeled in two ways: as a single measurement vector (SMV) problem and as a multiple measurement vector (MMV) problem.

A. SINGLE MEASUREMENT VECTOR CSMUD

In SMV model the CSMUD problem is formulated on symbol level where the activity detection is carried out for each symbol interval. The received signal after affected by AWGN noise and channel fading is given in frequency domain as

$$\begin{aligned} \mathbf{y} &= \mathbf{S}\mathbf{H}\mathbf{x} + \mathbf{w} \\ &= \mathbf{A}\mathbf{x} + \mathbf{w}, \end{aligned} \quad (7)$$

where $\mathbf{S} \in \mathbb{C}^{M \times N}$ consists of the spreading sequences of N users, $\mathbf{H} \in \mathbb{C}^{N \times N}$ is a diagonal matrix which consists of the channel coefficients of the users, $\mathbf{x} \in \mathbb{C}^{N \times 1}$ is the multiuser signal and $\mathbf{w} \in \mathbb{C}^{M \times 1}$ is the Gaussian noise. A zero element of vector \mathbf{x} represents an inactive user. The matrix, $\mathbf{A} \in \mathbb{C}^{M \times N}$ is the sensing matrix which consists of the combination of the spreading sequences and channel coefficients.

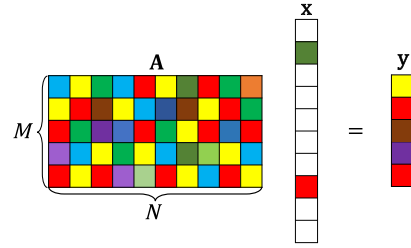


FIGURE 2. SMV based compressive sensing model for non-orthogonal multiple access.

In matrix form the SMV based CSMUD model is shown in Figure 2.

Using OMP to solve CSMUD for SMV model, at each iteration the active user is detected as the index of the maximally correlated column of the sensing matrix, \mathbf{A} , with the residual, \mathbf{r} (initialized to \mathbf{y} and updated in each iteration). The corresponding data symbol of the active user is then estimated using least square estimation.

B. MULTIPLE MEASUREMENT VECTOR CSMUD

In mMTC, when a node is active, it transmits more than one symbol at a time. This fact is used in modeling the CSMUD as an MMV model where it is assumed that the data frame consists of L symbols. The received data matrix is given in frequency domain as

$$\begin{aligned} \mathbf{Y} &= \mathbf{S}\mathbf{H}\mathbf{X} + \mathbf{W} \\ &= \mathbf{A}\mathbf{X} + \mathbf{W}, \end{aligned} \quad (8)$$

where $\mathbf{W} \in \mathbb{C}^{M \times L}$ is the Gaussian noise. $\mathbf{X} \in \mathbb{C}^{N \times L}$ consists of the modulated symbols of N users. Each row of \mathbf{X} represents L symbols of a user while each column consists of the symbols of all users at a time. The inactive user is represented by all zero row of the matrix. Figure 3 shows the MMV based CSMUD in matrix form.

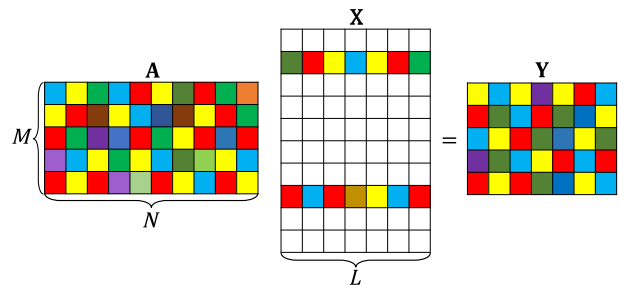


FIGURE 3. MMV based compressive sensing model for non-orthogonal multiple access.

In the case of MMV based CSMUD, at each iteration the activity detection is based on the average of the correlations of the columns of \mathbf{A} with the residual, \mathbf{R} (initialized to \mathbf{Y} and updated in each iteration), followed by the estimation of the corresponding data frame. The performance of MMV based CSMUD is better than the SMV based CSMUD for

the fact that in MMV case the correlations are averaged over L symbols.

IV. SEQUENCE BLOCK CSMUD

The performance of the conventional CSMUD depends on the maximum correlation, μ_{max} , between the spreading sequences assigned to the users. For a higher value of μ_{max} , the DER will be higher and vice versa. The maximum correlation, μ_{max} , is dependent on the length of the spreading sequence, i.e, the spreading factor. Increasing the spreading factor reduces the maximum correlation, μ_{max} , which improves the activity detection. However, higher spreading factor means using more radio resources, which is not desirable in an mMTC scenario. Therefore, to reduce the μ_{max} without increasing the spreading factor, we propose SB-CSMUD. It is an MMV based CSMUD scheme in which it is assumed that when a node is active it transmits L symbols, $\text{mod}(L, D) = 0$, where D is the number of sequence in a sequence block.

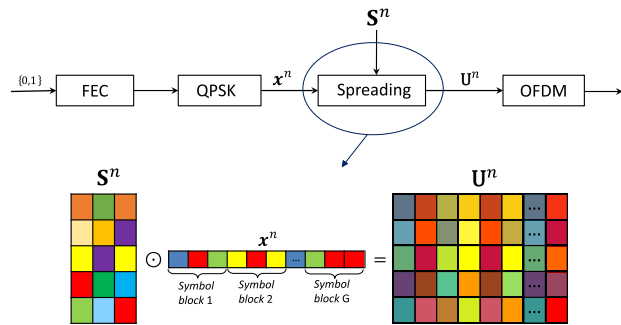


FIGURE 4. Processing at node n : \odot represents multiplication of first column of the S^n with first symbol of a symbol block of x^n , second column with second symbol and so on.

A. PROCESSING AT SENSOR NODE

In the proposed SB-CSMUD, instead of assigning a single sequence, a sequence block, $S^n \subset S, 1 \leq n \leq N$, of D sequences is assigned to each user which serves as the signature. The node processing in SB-CSMUD scheme is depicted in Figure 4. The signal after channel coding is modulated using quadrature phase shift keying. The modulated data frame is then spread using the assigned sequence blocks. The spreading process can be regarded as dividing the data frame into $G = L/D$ symbol blocks and spreading each symbol block using the user specific sequence block. The first symbol of each symbol block is spread using the first spreading sequence of the sequence block, the second using the second spreading sequence and so on. The resultant spread signal frames of all the N nodes $U^n \in \mathbb{C}^{M \times L}, 1 \leq n \leq N$, are then transmitted using orthogonal frequency division multiplexing.

B. SEQUENCE BLOCK DESIGN

A sensing matrix, $S \in \mathbb{C}^{M \times N}$, is generated by selecting random sequences from the unit circle such as $s_i(v) \sim \exp(2\pi v)$ with v being a uniform distribution on the interval $[0,1]$. For each user a block of D sequences are selected from the

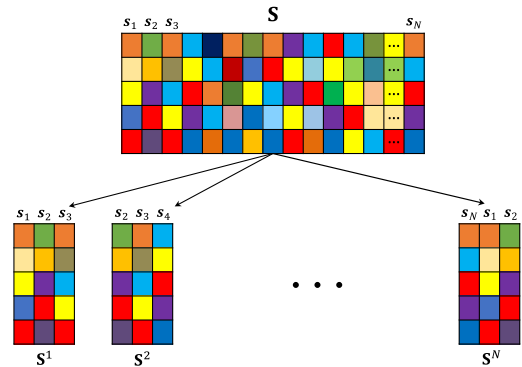


FIGURE 5. Selection of sequence blocks from sensing matrix .

sensing matrix S . The sequence block $S^n = [s_1^n, s_2^n, \dots, s_D^n]$, $1 \leq n \leq N$, is designed such that the sequences at the same index of all sequence blocks are unique, i.e., $s_d^i \neq s_d^j, i, j \in \{1, 2, \dots, N\}, i \neq j$, where s_d^j represents the d -th sequence of the j -th sequence block, $1 \leq d \leq D$. While several procedures are possible for choosing the sequences to form a sequence block, here for simplicity, a sliding window based procedure is employed to select D sequences from sensing matrix, S . In Figure 5, the design of sequence blocks for $D = 3$ is shown. The sequence block of node 1, $S^1 = [s_1, s_2, s_3]$, consists of the first three sequences of the spreading matrix, S . Similarly $S^2 = [s_2, s_3, s_4]$ and so on. Note that the total sequences used by SB-CSMUD are same as that of CSMUD. Owing to the random correlations among the columns of spreading matrix, the minimization of the maximum mutual correlation between the sequence blocks is sub-optimal. Therefore, the performance of the system can further be improved by designing the sequence blocks such that the maximum mutual correlation between the sequence blocks is minimized.

The sequence block is stored at the sensor node, thereby, increasing the memory requirement by D . However, the computational complexity of the spreading at the node as well as of the multiuser detection at the BS in SB-CSMUD is the same as that of CSMUD. The reason is that both CSMUD and SB-CSMUD process the same amount of symbols. The only difference is that in CSMUD all symbols use the same spreading sequence while in SB-CSMUD each symbol block uses a different spreading sequence from the sequence block.

C. PROBABILITY OF SUPPORT RECOVERY

The CSMUD is based on the OMP algorithm where at each iteration the activity and data are jointly detected. The support of signal y in Equation (7) is iteratively obtained as the index of the maximally correlated spreading sequence with the residual, r . The activity is detected as

$$I = \arg \max_{1 \leq j \leq N} |\langle \mathbf{a}_j, \mathbf{r} \rangle|$$

$$= \arg \max_{1 \leq j \leq N} \left(\sum_{k \in \Gamma} |\langle \mathbf{a}_j, \mathbf{a}_k \rangle| |x_k| + |\langle \mathbf{a}_j, \mathbf{w} \rangle| \right), \quad (9)$$

where \mathbf{a}_j represents the j -th column of the sensing matrix, \mathbf{A} , Γ is the set of the indexes of the active nodes, x_k is

data symbol of node k and $|\langle \cdot \rangle|$ represents the mutual correlation.

It is intuitive that the CSMUD recovers the support set if the minimum correlation between the spreading sequences of the active nodes and the received multiuser symbol is greater than the maximum correlation between the inactive nodes and the received multiuser symbol. In [33], it is shown that the OMP algorithm recovers the true support if

$$\min_{i \in \Gamma} \left(\sum_{k \in \Gamma} |\langle \mathbf{a}_i, \mathbf{a}_k \rangle| |x_k| + |\langle \mathbf{a}_i, \mathbf{w} \rangle| \right) \geq \max_{j \notin \Gamma} \left(\sum_{k \in \Gamma} |\langle \mathbf{a}_j, \mathbf{a}_k \rangle| |x_k| + |\langle \mathbf{a}_j, \mathbf{w} \rangle| \right). \quad (10)$$

The summation on the left hand side of Equation (10) also contains the self-correlation, $|\langle \mathbf{a}_i, \mathbf{a}_k \rangle|$, $i = k$, which is equal to 1. Therefore, we have

$$1 + \min_{i \in \Gamma} \left(\sum_{k \in \Gamma, i \neq k} |\langle \mathbf{a}_i, \mathbf{a}_k \rangle| |x_k| + |\langle \mathbf{a}_i, \mathbf{w} \rangle| \right) \geq \max_{j \notin \Gamma} \left(\sum_{k \in \Gamma} |\langle \mathbf{a}_j, \mathbf{a}_k \rangle| |x_k| + |\langle \mathbf{a}_j, \mathbf{w} \rangle| \right). \quad (11)$$

It is easy to understand that

$$1 + \min_{i \in \Gamma} \left(\sum_{k \in \Gamma, i \neq k} |\langle \mathbf{a}_i, \mathbf{a}_k \rangle| |x_k| + |\langle \mathbf{a}_i, \mathbf{w} \rangle| \right) \geq 1 - \max_{i \in \Gamma} \left(\sum_{k \in \Gamma, i \neq k} |\langle \mathbf{a}_i, \mathbf{a}_k \rangle| |x_k| + |\langle \mathbf{a}_k, \mathbf{w} \rangle| \right). \quad (12)$$

The relationship in (12) leads (11) to a stronger condition for the support recovery as follows

$$1 - \max_{i \in \Gamma} \left(\underbrace{\sum_{k \in \Gamma, i \neq k} |\langle \mathbf{a}_i, \mathbf{a}_k \rangle| |x_k|}_p + |\langle \mathbf{a}_i, \mathbf{w} \rangle| \right) \geq \max_{j \notin \Gamma} \left(\underbrace{\sum_{k \in \Gamma} |\langle \mathbf{a}_j, \mathbf{a}_k \rangle| |x_k|}_q + |\langle \mathbf{a}_j, \mathbf{w} \rangle| \right). \quad (13)$$

The activity of the nodes in mMTC is not known beforehand, therefore, without loss of generality p and q in Equation (13) can be considered as the sum of $K - 1$ and K correlations which maximizes the second term on the left hand side and the right hand side, respectively. Equation (13) can therefore be generalized to

$$1 - \max_{1 \leq i \leq N} \left(\sum_{k=1}^{K-1} \max_{1 \leq j \leq N} |\langle \mathbf{a}_i, \mathbf{a}_j \rangle| |x_j| + |\langle \mathbf{a}_i, \mathbf{w} \rangle| \right) \geq \max_{1 \leq i \leq N} \left(\sum_{k=1}^K \max_{1 \leq j \leq N} |\langle \mathbf{a}_i, \mathbf{a}_j \rangle| |x_j| + |\langle \mathbf{a}_i, \mathbf{w} \rangle| \right). \quad (14)$$

Taking the higher value for both sides of the equation, we have

$$\max_{1 \leq i \leq N} \left(\sum_{k=1}^K \max_{1 \leq j \leq N} |\langle \mathbf{a}_i, \mathbf{a}_j \rangle| |x_j| + \underbrace{|\langle \mathbf{a}_i, \mathbf{w} \rangle|}_\eta \right) \leq \frac{1}{2}. \quad (15)$$

Representing the set of indexes of the spreading sequences which maximizes the left hand side of Equation (15), by Ω and the corresponding correlations by μ , we have the condition for successful recovery as

$$\sum_{j \in \Omega} \mu_j |x_j| \leq \frac{1}{2} - \eta. \quad (16)$$

The probability of error in the activity detection, P_e , can therefore be defined as

$$P_e \leq \Pr \left\{ \sum_{j \in \Omega} \mu_j |x_j| > \frac{1}{2} - \eta \right\}. \quad (17)$$

By using Briesten inequality [36] we obtained the upper bound probability of error as

$$\Pr \left\{ \sum_{j \in \Omega} \mu_j |x_j| > \frac{1}{2} - \eta \right\} \leq \exp \left(\frac{-\left(\frac{1}{2} - \eta\right)^2}{2 \left(\sum_{j \in \Omega} E\{\mu_j^2 |x_j|^2\} + c\left(\frac{1}{2} - \eta\right)/3 \right)} \right) \leq \exp \left(\frac{-\left(\frac{1}{2} - \eta\right)^2}{2 \left(Kv + c\left(\frac{1}{2} - \eta\right)/3 \right)} \right), \quad (18)$$

where $E\{\mu_j^2 |x_j|^2\} \leq v$ and $\Pr\{\mu_j |x_j| \leq c\} = 1$. It is assumed that the transmit power of each node is one, i.e., $|x_j| = 1, \forall j$. However, there are only K nodes active at a time, therefore, the remaining $N - K$ nodes are represented by zero. The upper bounds c is therefore equal to μ_{max} and v is defined as

$$v = \frac{1}{N} \sum_{j=1}^N \mu_j^2 |x_j|^2 \leq \frac{K}{N} \mu_{max}^2. \quad (19)$$

The lower bound probability of successful support recovery for SMV based CSMUD, λ_{SMV} , is therefore stated as

$$\lambda_{SMV} \geq (1 - P_e) \Pr\left\{ \max_{1 \leq i \leq N} |\langle \mathbf{a}_i, \mathbf{w} \rangle| \leq \eta \right\}. \quad (20)$$

Combining Equation (18), (19) and (20) and assuming $\Pr\{\max_j |\langle \mathbf{a}_j, \mathbf{w} \rangle| \leq \eta\} = 1$, we have the lower bound success probability,

$$\lambda_{SMV} \geq 1 - \exp \left(\frac{-(1/2 - \eta)^2}{2 \left(\frac{K^2 \mu_{max}^2}{N} + \frac{\mu_{max}(1/2 - \eta)}{3} \right)} \right). \quad (21)$$

Equation (21) is based on SMV model where only a single multiuser signal is considered. However, in practice the active user transmits a sequence of symbols. Assuming that a user transmits L symbols per frame, the multiuser detection

problem is posed as an MMV compressive sensing problem. For the MMV case, the received signal of Equation (8), the decision of activity detection is based on the average of the correlations of the signature and the L received multiuser symbols. The success probability for MMV based CSMUD is therefore given as

$$\lambda_{\text{MMV}} \geq \frac{1}{L} \sum_{l=1}^L \left(1 - \exp \left(\frac{-(1/2 - \eta_l)^2}{2 \left(\frac{K^2 \mu_{\max}^2}{N} + \frac{\mu_{\max}(1/2 - \eta_l)}{3} \right)} \right) \right), \quad (22)$$

where η_l is the correlation between the l -th symbol of the frame and the Gaussian noise. The performance of the MMV based CSMUD is better than that of the SMV case due to the fact that every symbol in MMV case experiences a different Gaussian noise which introduces a diversity in the correlations between the spreading sequences and the received multiuser signals.

SB-CSMUD is an MMV based multiuser detection in which along with the diversity introduced by noise, the maximum correlation between the signatures is also reduced. The received signal after affected by the additive white Gaussian noise and channel fading is given in frequency domain as

$$\begin{aligned} \mathbf{Y} &= \sum_{n=1}^N \text{diag}(\mathbf{h}^n) \mathbf{S}^n \odot \mathbf{x}^n + \mathbf{W} \\ &= \sum_{n=1}^N \mathbf{B}^n \odot \mathbf{x}^n + \mathbf{W}, \end{aligned} \quad (23)$$

where,

$$\mathbf{B}^n \odot \mathbf{x}^n = [\mathbf{B}_1^n \mathbf{x}_1^n, \mathbf{B}_2^n \mathbf{x}_2^n, \dots, \mathbf{B}_D^n \mathbf{x}_D^n, \mathbf{B}_1^n \mathbf{x}_{D+1}^n, \dots, \mathbf{B}_D^n \mathbf{x}_{2D}^n], \quad (24)$$

$\mathbf{S}^n \in \mathbb{C}^{M \times D}$ is the spreading sequence block, $\mathbf{h}^n \in \mathbb{C}^{M \times 1}$ is the node and subcarriers specific channel coefficients, $\mathbf{x}^n \in \mathbb{C}^{1 \times L}$ is the data frame, $\mathbf{B}^n \in \mathbb{C}^{M \times D}$ is the combination of the channel and the spreading influences of the sequence block n and \mathbf{B}_d^n represents the d -th sequence in sequence block n . Note that for SB-CSMUD, the frame size, L , is selected such that $\text{mod}(L, D) = 0$. The sequence block serves as a signature for the node at the receiver, where the activity is detected based on the mean of the correlations between the sequence blocks and the received signal \mathbf{Y} , as

$$I = \arg \max_{1 \leq j \leq N} \left(\frac{D}{L} \sum_{l=1}^{L/D} \sum_{k \in \Gamma} |\langle \mathbf{B}^j, \mathbf{B}^k \rangle| \mathbf{x}_l^k + |\langle \mathbf{B}^j, \mathbf{W}_l \rangle| \right), \quad (25)$$

where

$$|\langle \mathbf{B}^j, \mathbf{B}^k \rangle| = \frac{1}{D} \sum_{d=1}^D \frac{|\langle \mathbf{B}_d^j, \mathbf{B}_d^k \rangle|}{\|\mathbf{B}_d^j\| \|\mathbf{B}_d^k\|}, \quad (26)$$

$$|\langle \mathbf{B}^j, \mathbf{W}_l \rangle| = \frac{1}{D} \sum_{d=1}^D \frac{|\langle \mathbf{B}_d^j, \mathbf{W}_{ld} \rangle|}{\|\mathbf{B}_d^j\| \|\mathbf{W}_{ld}\|}, \quad (27)$$

and

$$\mathbf{x}_l^k = \frac{1}{D} \sum_{d=1}^D |\mathbf{x}_{ld}^k| = 1, \quad \forall l \quad (28)$$

where \mathbf{W}_{ld} represent the random noise at the d -th sequence of the l -th symbol block and \mathbf{x}_l^k is the l -th symbol block of the k -th node.

The success probability of support recover for SB-CSMUD is given as

$$\lambda_B \geq \frac{D}{L} \sum_{l=1}^{L/D} \left(1 - \exp \left(\frac{-(1/2 - \eta_l^B)^2}{2 \left(\sum_{j \in \Omega_j^B} \mathbb{E}\{(\mu^{\mathbf{B}^j} \mathbf{x}_l^j)^2\} + \frac{c_B(\frac{1}{2} - \eta_l^B)}{3} \right)} \right) \right), \quad (29)$$

where Ω_j^B and $\mu^{\mathbf{B}^j}$ are the block counterparts of Ω_j and μ_j in Equation (17), respectively and

$$\begin{aligned} c_B &= \mu_{\max}^B \mathbf{x}_l^k \\ &= \max_{1 \leq i \neq j \leq N} |\langle \mathbf{B}^i, \mathbf{B}^j \rangle|. \end{aligned} \quad (30)$$

Similarly the upper bound of the correlation between the signature and the noise at the l -th symbol block is defined as

$$\eta_l^B = \max_{1 \leq j \leq N} |\langle \mathbf{B}^j, \mathbf{W}_l \rangle|. \quad (31)$$

As the selection of spreading sequences for the sequence blocks is based on sliding window method of length D , at most two sequence blocks can have $D - 1$ common spreading sequences. Without loss of generality, let the first $D - 1$ correlations be the maximum correlations amongst the D correlations that constitutes $\mu^{\mathbf{B}^j}$. The upper bound v_B for the expectation $\mathbb{E}\{(\mu^{\mathbf{B}^j} \mathbf{x}_l^j)^2\}$ can be obtained as

$$\begin{aligned} v_B &= \mathbb{E} \left\{ \left(\frac{1}{D} \left(\sum_{d=1}^{D-1} \mu_{\max}^{\mathbf{B}_d} + \mu_{\max}^{\mathbf{B}_D} \right) \mathbf{x}_l^j \right)^2 \right\} \\ &= \frac{1}{D^2} \left(\frac{2}{N} \sum_{n=1}^{N/2} \left(\sum_{d=1}^{D-1} \mu_{\max}^{\mathbf{B}_d} \right)^2 + \frac{1}{N} \sum_{n=1}^N \left(\mu_{\max}^{\mathbf{B}_D} \right)^2 \right. \\ &\quad \left. + 2 \frac{2}{N^2} \sum_{n=1}^{N/2} \sum_{d=1}^{D-1} \mu_{\max}^{\mathbf{B}_d} \sum_{n=1}^N \mu_{\max}^{\mathbf{B}_D} \right) \mathbf{x}_l^j \end{aligned} \quad (32)$$

where $\mu_{\max}^{\mathbf{B}_d}$ represents the correlation between the sequences at the d -th index of the maximally correlated blocks. As there are only K simultaneously active nodes, \mathbf{x}_l^j is equal to 1 for only K nodes. For the remaining $N - K$ nodes $\mathbf{x}_l^j = 0$, which limits the summation in Equation (32) to only K terms. Ignoring the last term on the right hand side of Equation (32) which is nearly zero for large N , we have

$$v_B \leq \frac{K}{ND^2} \left(2 \left(\sum_{d=1}^{D-1} \mu_{\max}^{\mathbf{B}_d} \right)^2 + \mu_{\max}^{\mathbf{B}_D} \right). \quad (33)$$

For the parameters defined in (30), (31) and (33), the lower bound success probability of support recovery for SB-CSMUD, λ_B , is obtained as

$$\lambda_B \geq \frac{D}{L} \sum_{l=1}^{L/D} \left(1 - \exp \left(\frac{-(1/2 - \eta_l^B)^2}{2 \left(K\nu_B + \frac{\mu_{max}^B (\frac{1}{2} - \eta_l^B)}{3} \right)} \right) \right). \quad (34)$$

where η_l^B is the correlation of the l -th symbol block with noise.

From Equation (21) and (34), it can be observed that $\lambda_B \geq \lambda$ only if $\mu_{max}^B < \mu_{max}$. To show that μ_{max}^B is always less than μ_{max} , we rewrite Equation (30) as

$$\mu_{max}^B = \frac{1}{D} (\mu_{max}^{B_1} + \mu_{max}^{B_2}, \dots, \mu_{max}^{B_d}, \dots, + \mu_{max}^{B_D}). \quad (35)$$

Each sequence block consists of D unique sequences from sensing matrix, \mathbf{A} , therefore, only one correlation in Equation (35) can be equal to the maximum correlation μ_{max} while the other $D - 1$ correlations are less than μ_{max} . Let $\mu_{max}^{B_1} = \mu_{max}$, then μ_{max}^B can be stated as

$$\mu_{max}^B = \frac{1}{D} (\mu_{max} + \mu_{max}^{B_2}, \dots, \mu_{max}^{B_D}) < \mu_{max}. \quad (36)$$

Equation (36) shows that the μ_{max}^B will always be less than μ_{max} which consequently implies that lower bound success probability of the support recovery of SB-CSMUD will always be higher than that of conventional CSMUD.

D. PERFORMANCE GAIN

The gain in support recovery achieved by the proposed scheme can be utilized in several aspects

- To reduce the required bandwidth by reducing the number of subcarriers;
- To reduce the DER using the same resources;
- To accommodate more active users.

The required bandwidth, B_W for data rate R_b , coding rate, R_c and R_s bits per symbol, is given as

$$B_W = \frac{R_b}{R_c R_s} M. \quad (37)$$

The gain in the required bandwidth achieved by SB-CSMUD can be given as

$$G_{B_W} = \frac{R_b}{R_c R_s} \frac{(M - M_B)}{M}, \quad \text{such that } \lambda_B = \lambda, \quad (38)$$

where M_B is the length of the spreading sequences of the SB-CSMUD, which is equal to the number of subcarriers. Keeping all other parameters constant, the required bandwidth gain is solely dependent on the difference between M and M_B .

For OMP based CSMUD algorithms, the required number of subcarriers to ensure a failure probability less than α for some constant $C > 0$ is given in [22] as

$$M \geq CK \log(N/\alpha). \quad (39)$$

The M in Equation (39) increases linearly with K which is limited by the maximum correlation between the signatures as given in Equation (5). In SB-CSMUD the correlation between the signatures is reduced which can potentially allow more simultaneous active nodes. The possible increase in active nodes is denoted by $\Delta K = K_B - K$, where K_B is the number of simultaneously active nodes supported by SB-CSMUD. The ΔK can be used in two ways either to accommodate more active users or to reduce the required number of subcarriers at the same BER which results in a gain in the bandwidth saving. The required number of subcarriers for SB-CSMUD ensuring the same BER is obtained as

$$M_B \geq CK \log(N/\alpha) - C \Delta K \log(N/\alpha), \quad (40)$$

Substituting Equation (40) in Equation (38), we obtain the gain in bandwidth saving as

$$G_{B_W} = \frac{R_b C \Delta K \log(N/\alpha)}{R_c R_s M}. \quad (41)$$

The overall BER is also dependent on the LSER according to Equation (6). Therefore, by reducing the number of subcarriers, the LSER of the active nodes also increases which results in increasing the overall BER. Therefore, the reduction in the number of subcarriers is limited by the tolerance level of increase in the LSER of the active nodes. For the scenarios where the accurate support recovery is more important than the actual data such as in smart temperature sensing where the sensor node becomes active when the temperature exceeds certain limit, the proposed scheme can further reduce the subcarriers while keeping the same DER as that of the conventional.

E. HOMOGENEOUS PERFORMANCE

Random matrices are considered to give good performance in the compressive sensing reconstruction. Using random sensing matrices in OMP based CSMUD, one of the drawbacks is that the users might not have homogeneous performances in terms of LSER. It is because the performance is dependent on the correlations of the spreading sequences which are not homogeneous in a random matrix. The users that are maximally correlated are highly prone to errors while those with smaller mutual correlation have lower LSER. The non-homogeneity becomes more evident when the data frame is large as the whole frame gets affected.

In the proposed scheme each node uses D spreading sequences, therefore, they have a higher spreading diversity in the transmitted data frame. In the worst case only L/D symbols in the data frame can get affected by the higher mutual correlation. As discussed in Section IV-D, the remaining $L - L/D$ symbols will always have less correlation with other nodes' spreading sequences. The proposed SB-CSMUD scheme therefore guarantees a more homogeneous performance. Furthermore, the diversity introduced by using multiple sequences also gives a small improvement in the overall LSER of the system.

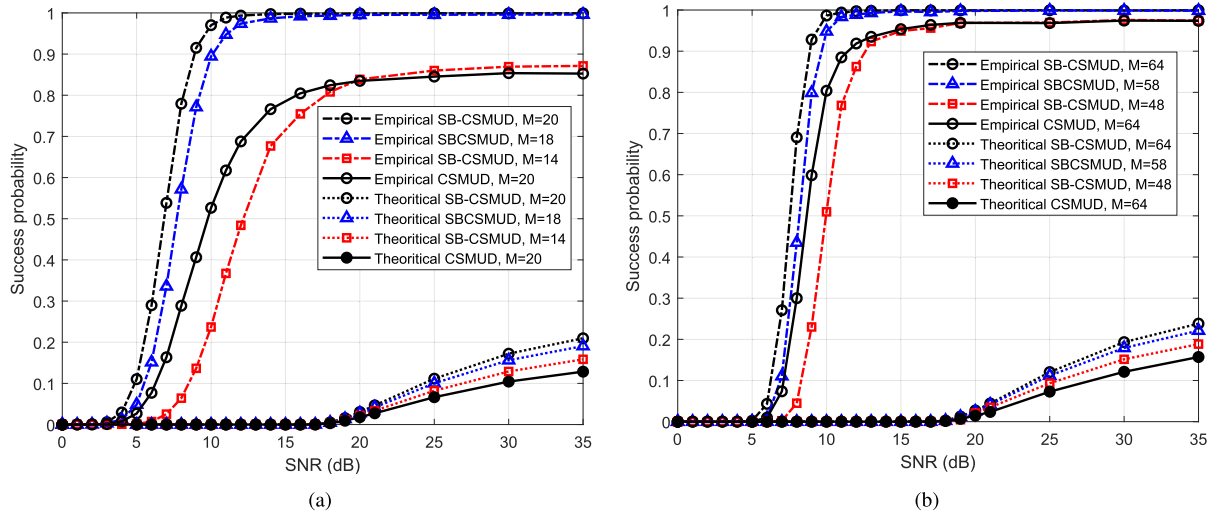


FIGURE 6. Probability of successful support recovery ($D = 4, L = 8$). (a) $K = 10; N = 60$. (b) $K = 30; N = 192$.

TABLE 1. Simulation parameters.

Number of Nodes	$N = 60, 192$
Length of spreading sequence	$M = 20, 64$
number of Active users	$K = 10, 30$
Overloading factor	$\rho = 3$
Length of frame	$L = 8, 20, 36$ symbols
Sequence block size	$D = 1 : 4$
Channel coding	Rate-1/2 Convolutional
Modulation	QPSK
Interleaver	Random
Delay spread length	1000 m

V. PERFORMANCE ANALYSIS

We analyzed the performance of the SB-CSMUD under different scenarios. For the performance analysis, we assume an exponentially decaying channel with a path loss constant of two. In addition, we assume that the channel remains same for the entire data frame and the channel state information is known at the receiver. The overloading factor is defined as $\rho = N/M$. The other simulation parameters are summarized in Table 1.

The lower bound probability of successful support recovery is shown in Figure 6. The probability of successful support recovery for the empirical results is defined as the ratio of the exact support recovery to the number of trials performed. The terms η and η_B are random quantities which cannot be calculated analytically, therefore, they are empirically calculated as the maximum correlation between the signatures and the noise in 10^4 trials.

Figure 6 shows the theoretical and empirical probability bounds of successful support recovery. In Figure 6(a), the probability bounds are shown for $M = 14, 18$ and 20 . It is evident that for $M = 20$, the success probability of the conventional CSMUD becomes flat at 0.85 while the success probability of SB-CSMUD is nearly one at $SNR > 20$ dB. The performance of the SB-CSMUD at $M = 18$ is nearly the

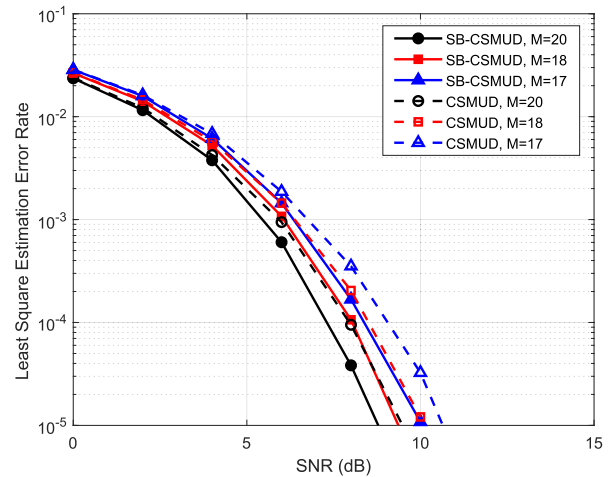


FIGURE 7. Effect of reducing subcarriers on the LSER of CSMUD and SB-CSMUD ($D = 4, N = 60, L = 8$).

same as that at $M = 20$ for $SNR > 15$ dB, which besides the improvement in the success probability over the CSMUD also results in a bandwidth gain of 10%. The performance curves at $M = 14$ shows that the bandwidth can further be reduced by 30% for $SNR > 20$ dB. It can be observed that the gap between the theoretical curves for CSMUD and SB-CSMUD at $M = 14$ is more than that in the empirical curves. The reason for this difference is that for theoretical results we consider the maximum value of η while in the empirical case the diversity in η is higher as each symbol experience a different noise. The same gain pattern can be observed in Figure 6(b) where the number of subcarriers are increased to $M = 64$ and total number of users to $N = 192$. It is clear that a 10% gain in bandwidth is achieved by reducing the subcarriers to $M = 58$ along with the gain in the performance. The subcarriers can be reduced to $M = 48$ to achieve the

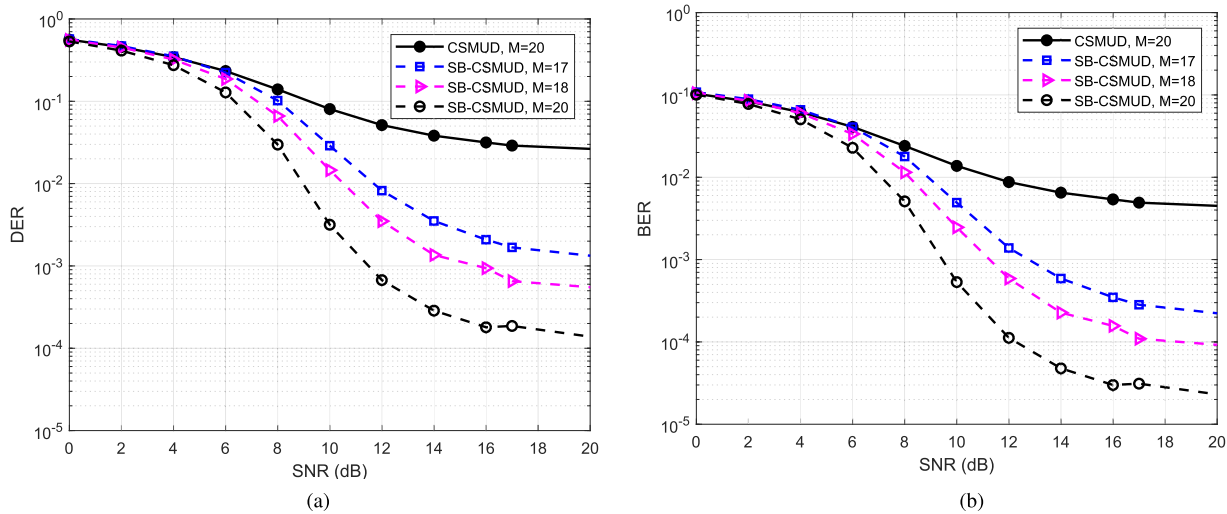


FIGURE 8. Performance comparison of CSMUD and SB-CSMUD ($K = 10, D = 4, N = 60, L = 8$). (a) Detection error rate. (b) Bit error rate.

same performance as that of CSMUD at $SNR \geq 20$ dB. The results in Figure 6 show that the proposed solution is feasible for small as well as for large number of nodes.

In Figure 6, it is shown that by using the SB-CSMUD we can reduce the required bandwidth to achieve the same activity detection. However, as the LSER also depends on the number of subcarriers, we have to consider the effect of reducing the subcarriers on the LSER. Figure 7 depicts the effect of reducing the subcarriers on the LSER. The simulations are carried out for known activity where the information about the active nodes are known at the BS, therefore, the BER constitutes only the LSER. From the figure, it is clear that as M decreases, the LSER increases for both CSMUD and SB-CSMUD. However, the reduction in the LSER of the SB-CSMUD is less than that of the CSMUD. The difference in the degradation rate comes from the diversity introduced by using D spreading sequences in SB-CSMUD. In CSMUD the effect of the highly correlated sequences remain the same for all the frame, while in SB-CSMUD, only L/D symbols in the data frame get affected, therefore, the overall LSER is improved. Due to this improvement, the LSER of the SB-CSMUD at $M = 18$ is approximately same as that of the CSMUD at $M = 20$, justifying the 10% gain in the bandwidth achieved by SB-CSMUD.

The overall performance gain of the SB-CSMUD in terms of DER and BER is demonstrated in Figure 8. At $M = 20$ the DER of the SB-CSMUD is lower than that of the CSMUD by two order of magnitude as shown in Figure 8(a) for $SNR > 15$ dB. The same gain pattern is observed in the overall BER curves in Figure 8(b). It is clear from Figure 8 that the major contribution in the degradation of the BER of the CSMUD comes from the detection errors. A single error in activity detection causes the whole frame in error as also shown in Equation (6). The SB-CSMUD primarily reduces the DER, which consequently reduces the overall BER.

The SB-CSMUD enhances the spectrum efficiency by reducing the number of subcarriers as shown in Figure 8. For $M = 18$, a gain of 1.5 order of magnitude in DER is achieved for SB-CSMUD at $SNR = 20$ dB. The reduction in subcarriers is equivalent to reducing the required bandwidth by 10% besides a gain of 1.5 order of magnitude in DER. In Figure 8, it can be observed that the subcarriers can further be reduced as even at $M = 17$ a gain of more than one order of magnitude is achieved. The property of support recovery using smaller number of subcarriers is of great interest in certain mMTC scenario where the activity detection is more important than the actual data.

Figure 9 presents the impact of the sequence block size, D , on the performance. As D increases, the maximum correlation, μ_{max}^B , decreases due to the averaging of several correlations. The reduction in maximum correlation results in reduction of the DER as shown in Figure 9(a) and consequently the BER in Figure 9(b). It can also be seen that the improvement in DER is not linear with the D . The gain in DER from $D = 1$ to $D = 2$ is more than that from $D = 2$ to $D = 3$. The reason for this is that v_B also increases with D which affects the gain in DER.

Figure 10 shows the relationship between the performance and the size of the frame. For CSMUD, a gain of one magnitude in DER is achieved at $SNR = 20$ dB for increasing $L = 8$ to $L = 20$ as shown in Figure 10(a). In case of SB-CSMUD the gain is significantly higher and no detection error is observed for $SNR > 8$ dB. The performance gain comes from the averaging of the correlations over multiple symbols for CSMUD and over multiple blocks for SB-CSMUD. In Equation (21) and (34) it can be seen that if all the L symbols of CSMUD and L/D blocks of SB-CSMUD experience the same noise, then the size of L will not affect the performance. However, in practice, the noise can never be the same for all symbols. Owing to the diversity introduced

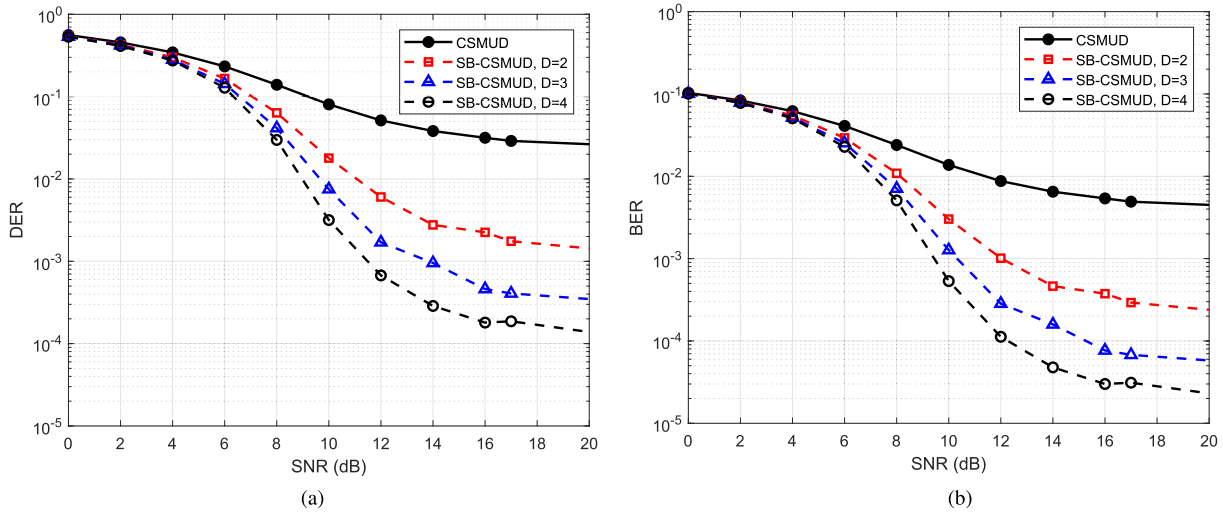


FIGURE 9. Effect of the sequence block size, D ($K = 10, M = 20, N = 60, L = 8$). (a) Detection error rate. (b) Bit error rate.

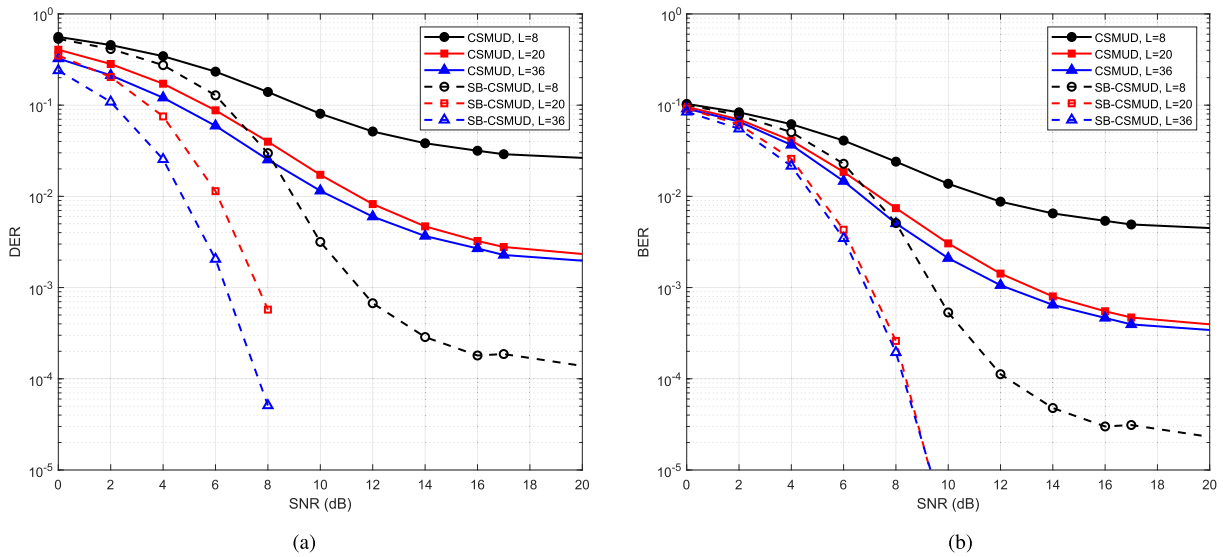


FIGURE 10. Effect of increasing frame size, L ($D = 4, K = 10, M = 20, N = 60$). (a) Detection error rate. (b) Bit error rate.

by the random noise, a significant gain in DER is achieved. From $L = 20$ to $L = 36$, the gain in DER is small for both CSMUD and SB-CSMUD due to the fact that the diversity becomes nearly same for further increasing the frame size. It can also be observed in Figure 10(b) that the BER improves with improvement in DER, however, from $L = 20$ to $L = 36$, the BER for SB-CSMUD is almost the same particularly for $SNR > 8$ dB. It is for the reason that no error is introduced by the error in the activity detection and further increasing the frame size will not affect the BER.

The relationship between the performance and the number of active nodes is demonstrated in Figure 11. For less sparse signal, the number of active users is higher, which contributes in increasing the multiple access interference, thereby, degrading the performance. It can be seen

in Figure 11(a) that the DER of the CSMUD is at least 10^{-2} even at $K = 8$. On the other hand due to the more efficient activity detection of SB-CSMUD, the DER of SB-CSMUD is 10^{-3} even at $K = 12$, resulting in one order of magnitude gain in DER at $SNR = 20$ dB along with accommodating 50% more nodes. A similar trend of performance gain in BER can be observed in The effect of reducing the sparsity on the overall BER is shown in Figure 11(b). The BER also degrades with the increase in the number of active nodes. However, the BER performance curves show that the DER is the dominant cause of the overall BER degradation. It can be concluded from the Figure 11 that the SB-CSMUD is more resilient to multiple access interference and can give reasonable performance in situation where the number of simultaneously active nodes is higher.

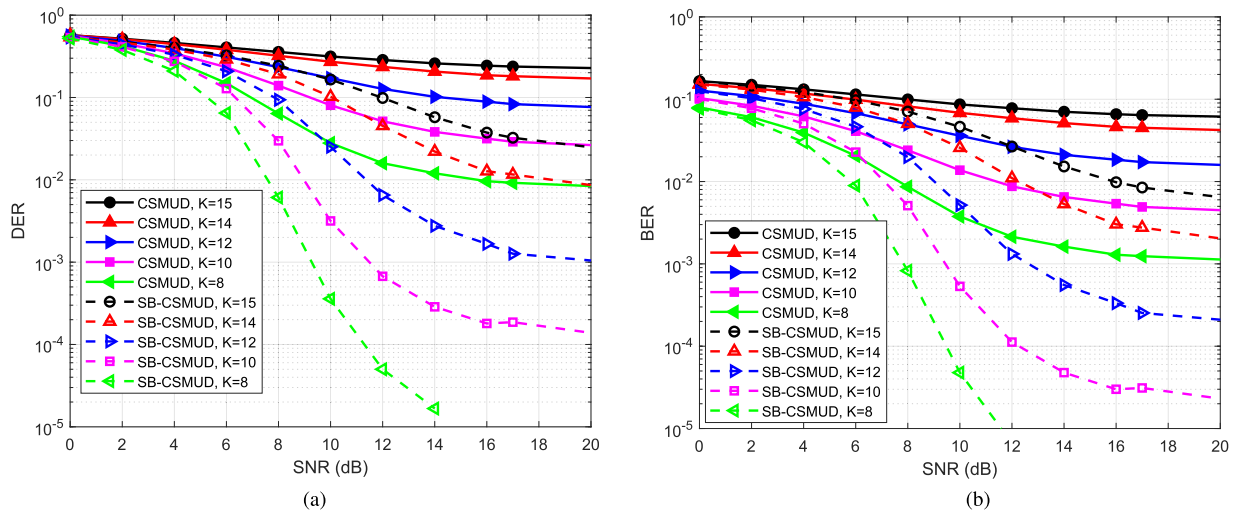


FIGURE 11. Effect of sparsity, K , on the performance ($M = 20, N = 60, D = 4, L = 8$). (a) Detection error rate. (b) Bit error rate.

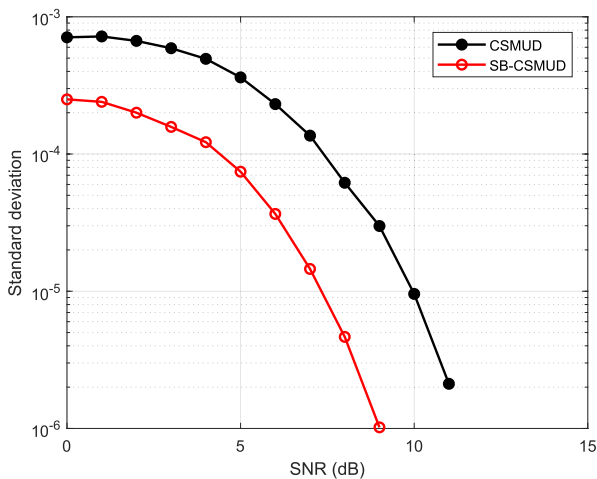


FIGURE 12. Standard deviation of the LSERs of the active nodes ($K = 10, M = 20, N = 60, D = 4$).

Figure 12 presents the advantage of providing homogeneous performance for all the nodes of the proposed SB-CSMUD over the conventional CSMUD. For the simulation, the maximally correlated sequences are assigned to the active users and the LSER of the individual users at known activity is obtained. In Figure 12 it is observable that the standard deviation of the LSERs of the active nodes in SB-CSMUD is substantially lower than that of the CSMUD, verifying that all the active nodes have approximately similar LSER. The reason for the improvement is discussed in subsection IV-E.

VI. CONCLUSION

In this paper we have proposed a non-orthogonal multiple access scheme with sequence block based CSMUD to enhance the spectrum efficiency, reduce the DER and BER, provide homogeneous performance for all nodes and to increase the overloading capability of the CSMUD.

The performance determining parameter of CSMUD, i.e., the maximum mutual correlation between the signatures, is reduced by exploiting the multi-symbol structure of the data frame. The proposed SB-CSMUD enhances the performance without increasing the length of the spreading sequence, thereby, improving the spectrum efficiency. It is shown that with SB-CSMUD, the required bandwidth can be reduced by at least 10%, which can further be reduced for applications where the accurate activity detection is the key requirement rather than accurate data estimation. Furthermore, it is also demonstrated that a more homogeneous performance for all users is achieved for the proposed SB-CSMUD. It is shown empirically as well as analytically that a significant improvement in the DER and the spectrum efficiency can be achieved without increasing the number of subcarriers. In addition, the SB-CSMUD have the same computational complexity as that of the CSMUD at the only expense of increased memory of the node for hosting the sequence block.

In the proposed scheme the sequence block design is a naive sliding window based selection of the sequences from the spreading matrix. It will therefore be an interesting topic to investigate the selection of sequences based on the minimization of the mutual correlation between the sequence blocks.

REFERENCES

- [1] Z. M. Fadlullah, M. M. Fouda, N. Kato, A. Takeuchi, N. Iwasaki, and Y. Nozaki, "Toward intelligent machine-to-machine communications in smart grid," *IEEE Commun. Mag.*, vol. 49, no. 4, pp. 60–65, Apr. 2011.
- [2] D. Evans, "The Internet of Things: How the next evolution of the Internet is changing everything," CISCO, San Jose, CA, USA, White Paper 1, vol. 1, 2011, pp. 1–11. [Online]. Available: https://www.cisco.com/c/dam/en_us/about/ac79/docs/innov/IoT_IBSG_0411FINAL.pdf
- [3] J. Chamber, "Beyond the hype: Internet of Things shows up strong at mobile world congress," PC World, 2014.
- [4] Q. Zhang and F. H. P. Fitzek, "Mission critical IoT communication in 5G," in *Future Access Enablers for Ubiquitous and Intelligent Infrastructures*. Cham, Switzerland: Springer, 2015, pp. 35–41.

- [5] T. Wen and P. Zhu, "5G: A technology vision," Huawei Technol. Co. Ltd., Shenzhen, China, White Paper, Nov. 2013. [Online]. Available: https://www.huawei.com/ilink/en/download/HW_314849
- [6] E. Dahlman, S. Parkvall, and J. Sköld, *4G: LTE/LTE-Advanced for Mobile Broadband*. Amsterdam, The Netherlands: Elsevier, 2013.
- [7] Y. Chen and W. Wang, "Machine-to-machine communication in LTE-A," in *Proc. IEEE 72nd Veh. Technol. Conf. Fall (VTC-Fall)*, Sep. 2010, pp. 1–4.
- [8] R. Ratasuk, N. Mangalvedhe, A. Ghosh, and B. Vejlgaard, "Narrowband LTE-M system for M2M communication," in *Proc. IEEE 80th Veh. Technol. Conf. (VTC Fall)*, Sep. 2014, pp. 1–5.
- [9] S. M. R. Islam, N. Avazov, O. A. Dobre, and K.-S. Kwak, "Power-domain non-orthogonal multiple access (NOMA) in 5G systems: Potentials and challenges," *IEEE Commun. Surveys Tuts.*, vol. 19, no. 2, pp. 721–742, 2nd Quart., 2017.
- [10] B. Ling, C. Dong, J. Dai, and J. Lin, "Multiple decision aided successive interference cancellation receiver for NOMA systems," *IEEE Wireless Commun. Lett.*, vol. 6, no. 4, pp. 498–501, Aug. 2017.
- [11] R. Hoshyar, F. P. Wathan, and R. Tafazolli, "Novel low-density signature for synchronous CDMA systems over AWGN channel," *IEEE Trans. Signal Process.*, vol. 56, no. 4, pp. 1616–1626, Apr. 2008.
- [12] H. Nikopour and H. Baligh, "Sparse code multiple access," in *Proc. IEEE Int. Symp. Pers. Indoor Mobile Radio Commun. (PIMRC)*, Sep. 2013, pp. 332–336.
- [13] M. Alam and Q. Zhang, "Designing optimum mother constellation and codebooks for SCMA," in *Proc. IEEE Int. Conf. Commun. (ICC)*, May 2017, pp. 1–6.
- [14] M. Alam and Q. Zhang, "Performance study of SCMA codebook design," in *Proc. IEEE Wireless Commun. Netw. Conf. (WCNC)*, Mar. 2017, pp. 1–5.
- [15] S. Chen, B. Ren, Q. Gao, S. Kang, S. Sun, and K. Niu, "Pattern division multiple access—A novel nonorthogonal multiple access for fifth-generation radio networks," *IEEE Trans. Veh. Technol.*, vol. 66, no. 4, pp. 3185–3196, Apr. 2017.
- [16] Z. Yuan, G. Yu, W. Li, Y. Yuan, X. Wang, and J. Xu, "Multi-user shared access for Internet of Things," in *Proc. IEEE 83rd Veh. Technol. Conf. (VTC Spring)*, May 2016, pp. 1–5.
- [17] H. Zhu and G. B. Giannakis, "Exploiting sparse user activity in multiuser detection," *IEEE Trans. Commun.*, vol. 59, no. 2, pp. 454–465, Feb. 2011.
- [18] H. F. Schepker and A. Dekorsy, "Sparse multi-user detection for CDMA transmission using greedy algorithms," in *Proc. 8th Int. Symp. Wireless Commun. Syst.*, Nov. 2011, pp. 291–295.
- [19] F. Monsees, M. Woltering, C. Bockelmann, and A. Dekorsy, "Compressive sensing multi-user detection for multicarrier systems in sporadic machine type communication," in *Proc. IEEE 81st Veh. Technol. Conf. (VTC Spring)*, May 2015, pp. 1–5.
- [20] C. Bockelmann, H. F. Schepker, and A. Dekorsy, "Compressive sensing based multi-user detection for machine-to-machine communication," *Trans. Emerg. Telecommun. Technol.*, vol. 24, no. 4, pp. 389–400, 2013.
- [21] M. Alam and Q. Zhang, "Enhanced compressed sensing based multiuser detection for machine type communication," in *Proc. IEEE Wireless Commun. Netw. Conf. (WCNC)*, Apr. 2018, pp. 1–6.
- [22] J. A. Tropp and A. C. Gilbert, "Signal recovery from random measurements via orthogonal matching pursuit," *IEEE Trans. Inf. Theory*, vol. 53, no. 12, pp. 4655–4666, Dec. 2007.
- [23] S. Chen, S. A. Billings, and W. Luo, "Orthogonal least squares methods and their application to non-linear system identification," *Int. J. Control*, vol. 50, no. 5, pp. 1873–1896, 1989.
- [24] H. F. Schepker and A. Dekorsy, "Compressive sensing multi-user detection with block-wise orthogonal least squares," in *Proc. IEEE 75th Veh. Technol. Conf. (VTC Spring)*, May 2012, pp. 1–5.
- [25] A. T. Abebe and C. G. Kang, "Compressive sensing-based random access with multiple-sequence spreading for MTC," in *Proc. IEEE Globecom Workshops (GC Wkshps)*, Dec. 2015, pp. 1–6.
- [26] E. J. Candès and M. B. Wakin, "An introduction to compressive sampling," *IEEE Signal Process. Mag.*, vol. 25, no. 2, pp. 21–30, Mar. 2008.
- [27] S. S. Chen, D. L. Donoho, and M. A. Saunders, "Atomic decomposition by basis pursuit," *SIAM Rev.*, vol. 43, no. 1, pp. 129–159, 2001.
- [28] E. J. Candès and T. Tao, "Decoding by linear programming," *IEEE Trans. Inf. Theory*, vol. 51, no. 12, pp. 4203–4215, Dec. 2005.
- [29] B. Bah and J. Tanner, "Improved bounds on restricted isometry constants for Gaussian matrices," *SIAM J. Matrix Anal. Appl.*, vol. 31, no. 5, pp. 2882–2898, 2010.
- [30] E. J. Candès, "Compressive sampling," in *Proc. Int. Congr. Math.*, vol. 3, Madrid, Spain, 2006, pp. 1433–1452.
- [31] D. L. Donoho and X. Huo, "Uncertainty principles and ideal atomic decomposition," *IEEE Trans. Inf. Theory*, vol. 47, no. 7, pp. 2845–2862, Nov. 2001.
- [32] D. L. Donoho and M. Elad, "Optimally sparse representation in general (nonorthogonal) dictionaries via ℓ_1 minimization," *Proc. Nat. Acad. Sci. USA*, vol. 100, no. 5, pp. 2197–2202, 2003.
- [33] Z. Ben-Haim, Y. C. Eldar, and M. Elad, "Coherence-based performance guarantees for estimating a sparse vector under random noise," *IEEE Trans. Signal Process.*, vol. 58, no. 10, pp. 5030–5043, Oct. 2010.
- [34] T. T. Cai, L. Wang, and G. Xu, "Stable recovery of sparse signals and an oracle inequality," *IEEE Trans. Inf. Theory*, vol. 56, no. 7, pp. 3516–3522, Jul. 2010.
- [35] A. Dekorsy and K.-D. Kammeyer, "A new OFDM-CDMA uplink concept with M -ary orthogonal modulation," *Eur. Trans. Telecommun.*, vol. 10, no. 4, pp. 377–389, 1999.
- [36] G. Bennett, "Probability inequalities for the sum of independent random variables," *J. Amer. Stat. Assoc.*, vol. 57, no. 297, pp. 33–45, 1962.



MEHMOOD ALAM received the B.E. and master's degrees in communication systems engineering from the National University of Sciences and Technology, Pakistan, in 2011 and 2014, respectively. He is currently pursuing the Ph.D. degree with the Department of Engineering, Aarhus University, Denmark. His research interests include the area of wireless communication, compressive sensing, 5G, and machine-type communication.



QI ZHANG received the M.Sc. and Ph.D. degrees in telecommunications from the Technical University of Denmark, Denmark, in 2005 and 2008, respectively. She is currently an Associate Professor with the Department of Engineering, Aarhus University, Denmark. Besides her academic experiences, she has various industrial experiences. Her research interests include mission critical communication, compressive sensing, Internet of Things, 5G and body area network, and network coding.

She is serving as an Editor for *EURASIP Journal on Wireless Communications and Networking*. She was the Co-Chair of the Co-operative and Cognitive Mobile Networks Workshop in the ICC Conference 2010–2015 and was a TPC Co-Chair of BodyNets 2015.

• • •